A Narrowband Ultrasonic Ranging Method for Multiple Moving Sensor Nodes

Karalikkadan Ashhar[1], Md.Noor-A-Rahim[2], Mohammad Omar Khyam[3] and Cheong Boon Soh[1]

***Abstract*—Accurate ranging using narrow-band ultrasonic transducers in small-scale environments can be used for indoor localization, human motion capture and robotic navigation. One of the main problems faced by the ultrasonic localization systems is the ranging error due to the Doppler shift. Existing methods for Doppler correction employ a bank of matched filters at the receiver end which is computationally intense and complex. On the other hand, enabling multiple access for the ultrasonic localization systems is a challenging task due to multiple access interference. We propose a method to measure range between multiple ultrasonic mobile nodes and static anchors in which we track the Doppler-velocity and correct the errors between the transmitted and the received signals due to the Doppler effect. We utilize range-Doppler coupling to estimate the Doppler shift and adjust the range values calculated by correlation. In our method, a unique set of two chirp signals are used for each transmitter to get one sample reading. The simulation results show high ranging accuracy and robustness using the proposed method as the Doppler-velocity increases. A pendulum experiment was conducted to validate the method using narrowband ultrasonic sensors. The multiple access interference problem was tackled by orthogonal coding the chirp signals and Doppler-correction. An improvement in the ranging accuracy was observed over traditional methods using chirp signals without Doppler correction.**

***Index Terms*—Ultrasonic multiple access, Ultrasonic ranging, Doppler shift compensation.**

I. Introduction

MOTION tracking using cost-effective narrowband ultrasonic transducers has potential applications in rehabilitation [1] and indoor robot navigation [2], [3]. These applications demand high accuracy and data update rate along with simultaneous tracking of multiple mobile nodes. For tracking multiple moving ultrasonic nodes, multiple ultrasonic nodes need to emit signals simultaneously in the presence of the Doppler effect which requires a careful utilization of the available bandwidth. We present two ranging methods using chirp signals for Doppler correction. Current systems for indoor motion capture are based on optical sensors and reflective markers which need dedicated laboratories with controlled lighting conditions and are costly. The motion tracking systems using micro-electromechanical (MEMS) systems such as accelerometers and gyroscopes are affected by fluctuations in the offset values and error accumulation while performing integration of acceleration and angular velocity values to obtain position [4]. Multiple sensor fusion needs to be done using inertial sensors to get satisfactory tracking performance [5], [6], which increases the cost and complexity of the system. Magnetic sensors can be used along with inertial measurement units to obtain sub-centimeter accuracy [7]; however, the magnetic sensors are affected by the ferromagnetic materials present in typical indoor environments.

Time of Flight (ToF)- based sensors such as ultrasonic and ultrawideband (UWB) sensors can be exploited for getting three-dimensional (3D) coordinates of moving targets in a fixed coordinate system from the distances between the mobile and anchor nodes using some localization algorithms [8], [9]. Precise calculation of ToF requires accurate clock synchronization between the transmitter node and the receiver node. Wireless localization systems are prone to errors in clock synchronization which leads to errors in ToF. The error in the estimation of range can be given by, $\delta d = v \times \delta t$, where δt is the error in the time of flight and v is the velocity. Here, as the velocity of the wave increases, the error in the estimated range also increases. Hence slower waves such as ultrasound can withstand much more errors in ToF compared to electromagnetic waves. Cross-correlation of the received signal with the initially transmitted signal is considered a standard method for calculation of range. Frequency modulated linear chirps give better cross-correlation performance in time-varying fading channels compared to single-tone signals [10]. Polyvinylidene Fluoride (PVDF) [11], Electromechanical Film (EMFi) [12] and capacitive/piezoelectric Micromachined Ultrasonic Transducers (cMUTs/pMUTs) [13] can be used to design ultrasonic sensors with higher bandwidth which can provide better noise tolerance, data update rate and wireless channel multiple access using various signal processing methods such as Direct Sequence Spread Spectrum (DSSS) [14], [15], Frequency Hopping Spread Spectrum (FHSS) [16], [15], Code Division Multiple Access (CDMA) [17] etc. However, the cost of the system increases significantly and higher operating voltages make the system unfit for mobile and wearable applications. Spread spectrum signals were used along with narrowband ultrasonic sensors in [18]; however, the use of 1 kHz clock for the pseudo-random code increases the length of the transmitted signal which leads to limited data update rate for tracking. Narrowband ultrasonic sensors were used for tracking two moving mobile nodes attached to the feet of a walking human subject in [1]. However, the method to track more than two mobile nodes requires some chirp diversity coding so that all transmitters can transmit simultaneously. Orthogonal Frequency Division Multiplexing (OFDM) was

[1]School of Electrical and Electronic Engineering, Nanyang Technological University Singapore 639798; ashhar001@e.ntu.edu.sg; ecbsoh@ntu.edu.sg

[2]School of Computer Science, University College Cork, Ireland; noomy004@mymail.unisa.edu.au

[3]Department of Mechanical Engineering, Virginia Tech, VA, Blacksburg, 24060, USA; mok@vt.edu

implemented for multiple access using narrowband ultrasonic sensors in [8]; however, OFDM signals suffer from high peak to average power ratios. Also, the Doppler effect can disturb the orthogonality of the signals involved. Leaving guard bands between different orthogonal carrier frequencies to avoid interference demands more bandwidth. In [10], a chirp waveform diversity design for static transducers is explained. The signal transmitted by each transmitter was made up of sub-chirps and was optimized for maximum orthogonality. However, moving ultrasonic transducers introduces Doppler shift in the received signals and this affects not only the orthogonality of individual waveform but also the range measurements extracted. A bank of correlation receivers is used in many systems to estimate and correct the Doppler shift [19], [20] where the frequency of the transmitted signal is shifted in steps to find the maximum amplitude of the correlation of the transmitted signal with the received signal. These systems are not computationally efficient as a lot of correlation operations need to be performed. A system which uses pilot carriers with a higher transmission power was explained in [21]. Even though this avoids the need for a bank of matched filters, altering a particular frequency component decreases the correlation performance and we also need higher resolution in the frequency domain to achieve high accuracy tracking.

We propose a method for estimation and correction of Doppler effect which does not use a bank of matched filters, instead requires only two correlations for estimating one sample point. The contribution of this paper is two folds; initially, we propose a method in which more than two ultrasonic signals can be transmitted simultaneously in the presence of Doppler effect. In the second method, a Doppler-velocity estimation algorithm is proposed which successively tracks and adjusts the errors due to the Doppler effect. We exploit the range-Doppler coupling [22] to estimate the Doppler shift and correct the range using the estimated velocity in each step.

The rest of the paper is organized as follows: Section II explains the basic ranging and correlation of signal for the coherent reception. In Section III, the generation of orthogonal chirp signals and the chirp signal modulation is explained. Section IV describes the proposed methods for Doppler corrections. Section V explains the simulation experiments conducted and the results. Section VI explains the experimental procedures with ultrasonic sensors. Section VII explains the results from experiments and Section VIII concludes the work with some ideas for future work.

II. Ranging between mobile and static nodes

An ultrasonic localization system can be designed with an active or passive mobile node architecture. In the active mobile node architecture, the mobile nodes send signals which will be captured by anchor nodes and analyzed for range estimation. For systems with the number of mobile nodes less than or equal to the number of anchor nodes, the active mobile node architecture is desired as the number of simultaneously transmitted signals and thus the multiple access interference and the power consumption is lower compared to passive mobile node architecture. Also, the data collection in a central server will be easier with active mobile node architecture if wired connections are to be employed. This paper represents the ranging between four mobile nodes and one receiver (see the setup shown in Fig. 1 in which multiple mobile transmitters are attached on a moving pendulum and the static receiver acquires the signal). The velocity of the moving transmitters with respect to the receivers introduces a Doppler shift in the frequency of the received signals. Let $\hat{S_n(t)}$ be the frequency shifted transmitted signal in time domain corresponding to the originally transmitted signal $S_n(t)$. The received signal at one receiver can be represented by:

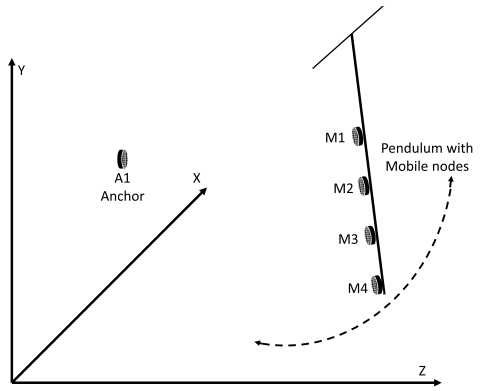

Fig. 1. A representation of the setup to measure range from one anchor node to four mobile nodes on a pendulum swinging in X-Y plane.

$$R(t) = \sum_{n=1}^{N} \hat{S_n(t)} * I_n(t) + n(t) \tag{1}$$

Where, $\hat{S_n(t)}$ represents the Doppler shifted signal transmitted by n^{th} transmitter, $I_n(t)$ represents the impulse response of the ultrasonic channel which accounts for the multi-path components as well and $n(t)$ represents the additive white gaussian noise. For coherent reception and ToF calculation at the anchor nodes, we take the correlation of the transmitted wave with the received signal. The correlation of $R(t)$ with the k^{th} transmitted waveform yields:

$$\begin{aligned} C_k(t) &= \Big[\sum_{n=1}^{N} \hat{S_n(t)} * I_n(t) + n(t)\Big] \star S_k(t) \\ &= \Big[\hat{S_k(t)} * S_k(-t)\Big] * I_k(t) \\ &+ \Big[\sum_{n\neq k} \hat{S_n(t)} * S_k(-t)\Big] * I_n(t) + n(t) * S_k(-t) \end{aligned} \tag{2}$$

Where, $\star$ represents correlation operation and $*$ represents convolution operation. The ToF information is embedded in the first term of Equation 2, $\Big[\hat{S_k(t)} * S_k(-t)\Big] * I_k(t)$. In the absence of Doppler effect that is when the velocity of the mobile node is zero, this term becomes $\Big[S_k(t) * S_k(-t)\Big] * I_k(t)$. As velocity increases, the peak amplitude decreases and the time at which the peak happens also changes if linearly varying signal frequency is used for ranging. The second term in Equation 2 accounts for the multiple access interference. The ToF is estimated from the peak value of $C_k(t)$ and we convert the ToF to distance by multiplying with the velocity

of the wave. The velocity of the ultrasound is given by $v = 331.5 + 0.6 \times T$, where T is the ambient temperature in degree Celsius. We conduct the experiments at 23^oC room temperature. The temperature correction can be automated by introducing a temperature sensor in the system, and in that case, we do not require any re-calibration once the system is set up. The dependence of sound velocity on humidity and altitude is negligible.

III. Signal Design

Linear chirp sequences are used in the proposed ranging system to obtain good correlation characteristics. Unlike broadband sensors such as EMFi and PVDF narrowband piezoelectric ceramic sensors are cheaper (<USD $50), lighter and works with low voltage (<20v). However, these sensors have a narrow bandwidth of around 2-4 kHz centered at its resonance frequency. Hence, we selected the narrow bandwidth of 38-42 kHz for our experiments. Sensors with higher bandwidth can provide better results with increased complexity and cost. The narrow bandwidth is more critical for the transmitters as there are commercially available MEMS microphones which can receive broadband signals using low-power; however, transmitters need high DC-bias voltage. Two sets of chirp sequences were created by concatenating linear sub-chirps with same chirp lengths and bandwidths and having different starting and stopping frequencies. The first set contains only sub-chirps with linearly increasing frequencies while the second set contained only sub-chirps with linearly decreasing frequencies. An optimization method was used for selection of the sequence of sub-chirps. The steps for signal design are briefly explained here [10].

1) Step-1: Linear up and down chirps were generated using the Equation 3.

$$\begin{aligned} S_u(t) &= \cos\Big\{2\pi\Big(f_s t + \frac{(f_e - f_s)t^2}{2 \times T_s}\Big)\Big\} \quad 0 \le t \le T_s \\ S_d(t) &= \cos\Big\{2\pi\Big(f_e t - \frac{(f_e - f_s)t^2}{2 \times T_s}\Big)\Big\} \quad 0 \le t \le T_s \end{aligned} \tag{3}$$

Where, f_s and f_e are starting and ending frequencies and T_s represents the total signal duration.

2) Step-2: Divide the up and down chirps into N sub-chirps using Equation 4.

$$\begin{aligned} Y_{u_n}(t) &= \cos\Big\{2\pi\Big(f_{s_n} t + \frac{(f_{e_n} - f_{s_n})t^2}{2 \times T_c}\Big)\Big\} \quad 0 \le t \le T_c \\ Y_{d_n}(t) &= \cos\Big\{2\pi\Big(f_{e_n} t - \frac{(f_{e_n} - f_{s_n})t^2}{2 \times T_c}\Big)\Big\} \quad 0 \le t \le T_c \end{aligned} \tag{4}$$

Where, $f_{s_n} = f_s + \frac{(n-1)(f_e - f_s)}{N}$, $f_{e_n} = f_{s_n} + \frac{(f_e - f_s)}{N}$, $n = 1, 2, ..N$ and $T_c = \frac{T_s}{N}$. We considered two scenarios: (1) $f_s =$ 38 kHz, $f_e =$ 42 kHz, $T_s =$ 12 ms and $N = 4$ so that each chirp-let stretches 1 kHz in 3 ms time. (2) $f_s =$ 37 kHz, $f_e =$ 43 kHz, $T_s =$ 12 ms and $N = 6$ so that each chirp-let stretches 1 kHz in 2 ms time.

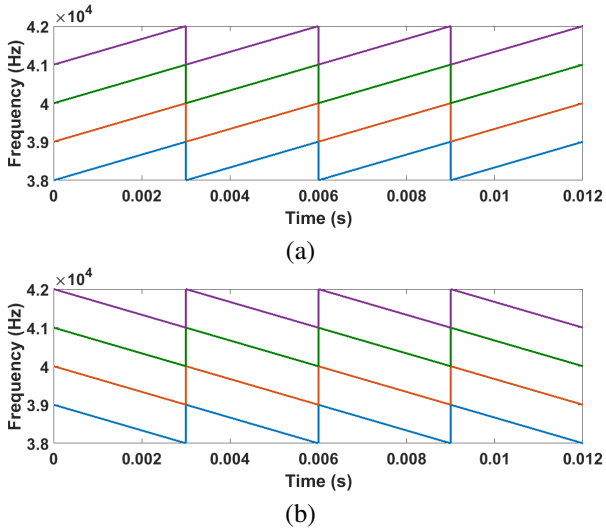

Fig. 2. Representation of (a) up chirp basis and (b) down chirp basis signals for the first scenario.

3) Step-3: Chirp basis signals are created for set-1 (up chirp) and set-2 (down chirp) using Equation 5.

$$\begin{aligned} \phi_{n,u}(t) &= \sum_{n=1}^{N} Y_{u_n}(t - (n-1)T_c) \\ \phi_{n,d}(t) &= \sum_{n=1}^{N} Y_{d_n}(t - (n-1)T_c) \end{aligned} \tag{5}$$

Fig. 2 shows the up chirp basis and down chirp basis.

4) Step-4: Generate N orthogonal unity height pulses. Construct a randomly circular shifted N unity height pulses which will be optimized using a trial and error method for maximum orthogonality.

$$\eta_{n,i}(t) = U(t) shift\Big((i_n - 1)T_c\Big) \tag{6}$$

Where, $i_n \in 1, 2...N$, $shift\Big(t\Big)$ represents circular shift by t and

$$U(t) = \begin{cases} 1 & 0 \le t \le T_c \\ 0 & T_c < t \le T_s \end{cases}$$

5) Step-5: Create orthogonal sets of N signals for the up sub-chirps. From the i sets of signals generated, j sets of N orthogonal signals are formed. An optimization algorithm was carried out to find the set of signals with minimum cross-correlation peak as well as minimum side-lobe peaks for auto-correlation. The maximum peak in the auto-correlation of a signal other than the main peak together with the maximum peak of cross-correlation with other signals in the set was minimized. Here we used an exhaustive search method with 10000 iterations to find the best candidate signal set which gives least multiple access interference when transmitted simultaneously. However, this is only a one-time search and once the set of signals are obtained, the same signals can be used for all the experiments.

$$s_{j,u}(t) = \sum_{n=1}^{N} \phi_{n,u}(t)\eta_{n,j}(t) \tag{7}$$

The value of $\eta_{n,j}(t)$ which provides maximum orthogonality was identified as $\eta_{n,j_{opt}}(t)$. The corresponding down sub-chirp signals are generated by Equation 8. Since the sweep directions of the chirp signals do not affect the correlation performance [23], we can use the same optimized set of unity height pulses to generate the set-2 signals using down sub-chirps. The set-1 signals optimized using the iterative optimization algorithm and the corresponding set-2 signals for four ultrasonic transducers are shown in Fig. 3.

$$s_{j,d}(t) = \sum_{n=1}^{N} \phi_{n,d}(t)\eta_{n,j_{opt}}(t) \tag{8}$$

IV. Proposed Method

Once two set of signals are ready, each transmitter transmits their corresponding signal from each set to calculate the range independently one after the other in each cycle of data acquisition. The total duration of one data acquisition cycle was set to 40 ms, out of which first 20 ms for ranging with the signal from set-1 and next 20 ms for ranging with the corresponding signal from set-2. The timeline for one ranging cycle is shown in Fig. 4. Two methods to obtain the accurate range measurements are explained here. From Equation 2, it can be seen that the Doppler shift introduces errors in both the first (ToF value) and second terms (multiple access error). The Doppler-effect shifts the frequency of the different transmitted signals in different amounts and this also increases the multiple access error. In the proposed methods, first method corrects only errors in ToF value while the second method estimates the Doppler-velocity and corrects both the errors. The proposed methods are explained here:

1) Mean-measurement method: In this method, we take the average value of the range measurements to remove the range-Doppler coupling effect. A similar method with only two mobile nodes were explained in [1] where the mean value of up- and down-chirp signal measurements are taken as an estimate of actual reading. However, the chirp signals were not coded and which limits the number of mobile nodes to two. In our method, we use coded chirp signals and mean value of signals from set-1 and set-2 are taken as the estimate of actual measurement. The actual range measurements can be estimated by Equation 9.

$$\begin{aligned} r_{1_n}(t) &= r_{0_n}(t) + \frac{\dot{r_n}(t) f_0 T_s}{B} \\ r_{2_n}(t) &= r_{0_n}(t) - \frac{\dot{r_n}(t) f_0 T_s}{B} \\ r_{0_n}(t) &= \frac{(r_{1_n}(t) + r_{2_n}(t))}{2} \end{aligned} \tag{9}$$

Where, $r_{1_n}(t)$, $r_{2_n}(t)$ and $r_{0_n}(t)$ represents the range estimated using signals from set-1, set-2 and the actual range value respectively for the n^{th} mobile node. The Doppler-velocity which is the velocity of mobile node along the line connecting the mobile node and the anchor node is represented by $\dot{r_n}(t)$. Centre frequency, $f_0 = (f_s + f_e)/2$ and bandwidth, $B = f_e - f_s$

2) Doppler-velocity correction method: In this method, the Doppler-velocity is estimated from range calculated using signals from set-1 and set-2 in each sampling instance and the template waveform for correlation at the receiver side is corrected for mismatch of received signals and originally transmitted signals. As the peak value of correlation at the receiver decreases due to the mismatch introduced by the Doppler effect, peaks due to multiple access interference can have higher values when compared to the main peak which leads to large errors in the measured range. Fig. 5 shows the flow chart for the method we used to compensate these errors during the coherent reception. In each step, the differential Doppler-velocity, $\Delta\dot{r_n}(t)$ can be calculated from Equation 9 by subtracting $r_{2_n}(t)$ from $r_{1_n}(t)$.

$$\Delta\dot{r_n}(t) = [r_{1_n}(t) - r_{2_n}(t)]\frac{B}{2f_0T_s} \tag{10}$$

At any point, if the estimated Doppler-velocity is above the maximum set Doppler-velocity, V_{dmax} or below the minimum set Doppler-velocity, V_{dmin}, The Doppler-velocity used for correction in the next step is reset to zero. The template signals for correlation at the receiver are corrected to account for the Doppler effect with the Doppler velocities obtained in previous step. The new chirp signals are generated using Equation 11 [24].

$$\begin{aligned} \hat{S_u}(t) &= \cos\Big\{2\pi\Big(b_n(t)f_s t + \frac{b_n(t)^2(f_e - f_s)t^2}{2 \times T_s}\Big)\Big\} \\ \hat{S_d}(t) &= \cos\Big\{2\pi\Big(b_n(t)f_e t - \frac{b_n(t)^2(f_e - f_s)t^2}{2 \times T_s}\Big)\Big\} \end{aligned} \tag{11}$$

Where, $b_n(t) = \frac{v}{(v + v_{d_n}(t - T_s))}$ and $0 \leq t \leq \frac{T_s}{b_n}$. The velocity of sound waves given by $v = 331.5 + 0.6 \times T$, T is the temperature and $v_d(n-1)$ is the estimated Doppler-velocity at the $(n-1)^{th}$ instance given by Equation 12.

$$v_{d_n}(t - T_s) = \sum_{i=0/r_s}^{t-T_s} \Delta\dot{r_n}(i) \tag{12}$$

Please note that when v_{d_n} is reset to zero at any point, the sum will be taken from that point, $t = r_s$. After correction, new basis signals are generated and new template signals for correlation are obtained from the already optimized symbols as explained in Section III. Finally, correlation is performed with new signals with both signals from set-1 and set-2 generated from the new chirp waves $\hat{S_u}(t)$ and $\hat{S_d}(t)$. The average value of range estimated from both of them is taken as the final range measurement.

As an example, consider the scenario-1 explained earlier with four transmitters. Let $v_{d_n}(t - 2T_s)$=1 m/s. At time, t, let the range obtained using signal from set-1, $r_{1_n}(t)$=1.05 m and from set-2, $r_{2_n}(t)$=1 m. Then using Equation 10, $\Delta\dot{r_n}(t)$=0.208 m/s and $v_{d_n}(t - T_s)$=1.208 m/s. The correction factor for chirp signals, $b_n(t)$= 0.996.

V. Simulation Results

A customized ranging environment with four transmitters and one receiver was simulated in Matlab. The transmitters were made to move towards and away from the receiver

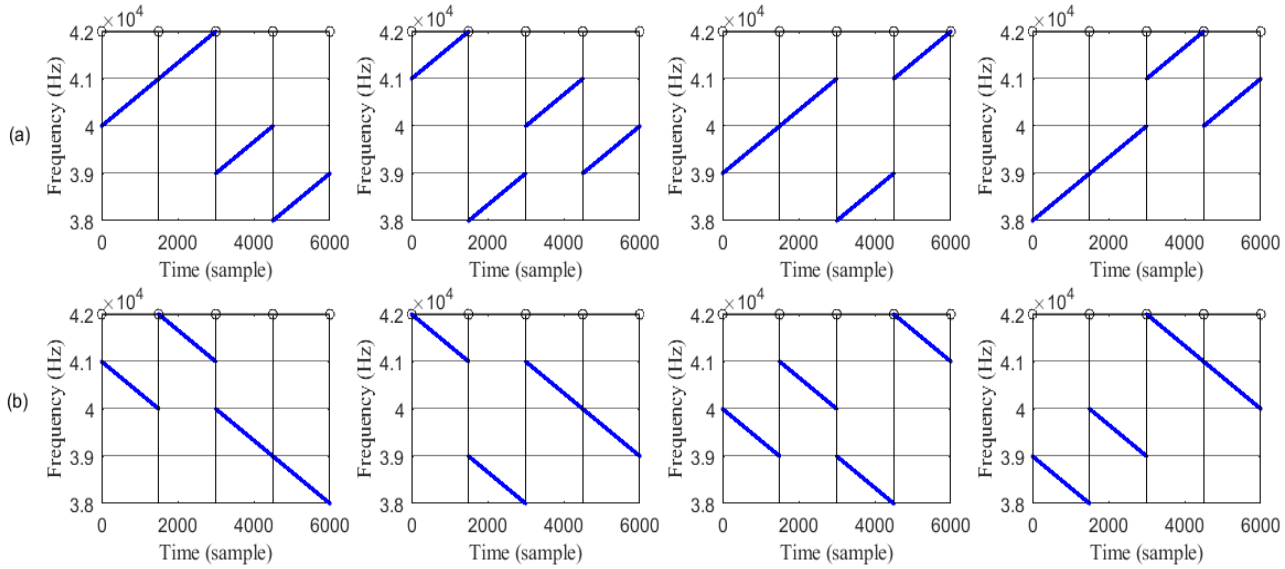

Fig. 3. (a) Four signals in set-1 after optimization and (b) the corresponding signals in the set-2

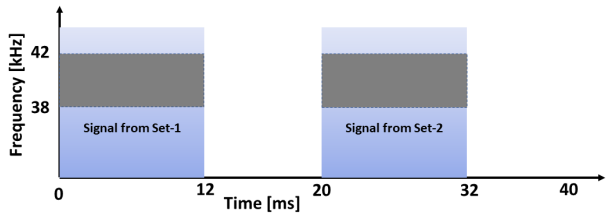

Fig. 4. Representation of one ranging cycle

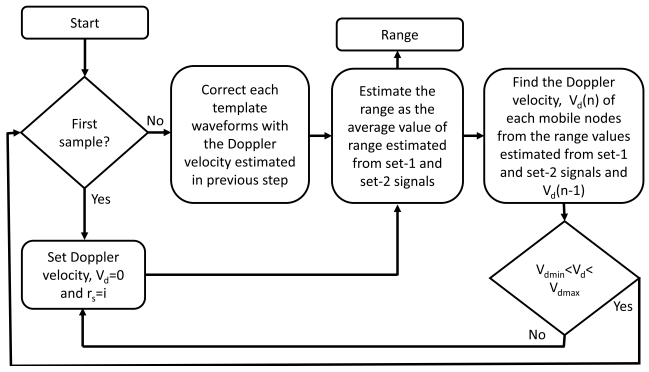

Fig. 5. Flow chart showing the steps involved in the coherent reception during Doppler-velocity correction method

periodically with velocities increasing linearly from 0 m/s to $+v_{max}$ m/s and then decreasing to $-v_{max}$ m/s. We started the movement of different transmitters at different times with random starting points. The plot of the velocities of four mobile nodes when v_{max}=1 m/s are shown in Fig. 6. The Doppler shifts in the received signals were simulated according to the velocities of the transmitters. The Doppler velocities are approximately the same as the velocities in Fig. 6 as the movement was simulated in the propagation direction of the wave. The simulated wireless channel was subjected to one multipath at random positions with a reflection coefficient of 0.4. The

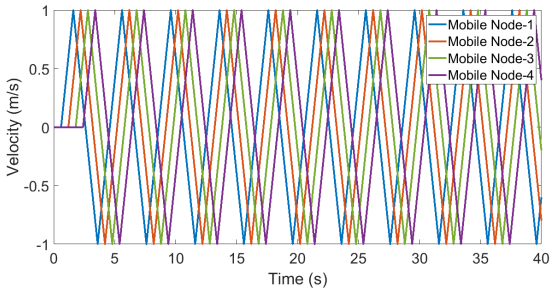

Fig. 6. Simulated Doppler-velocity of each mobile node

minimum separation between the LOS and NLOS was always kept greater than $1/B$ seconds which is the maximum range resolution for chirp signals [25]. To evaluate the performance of the ranging methods explained in Section IV, we considered two scenarios with four and six number of mobile nodes as mentioned in Section-III. In each case, the simulation was run for 1000 times and the mean value of error was calculated. All transmitters were made to send the signal assigned to it simultaneously while they are moving. The sampling rate of the system was set to 500000 samples per second. Two SNR levels were considered during simulations: (1) Additive White Gaussian Noise (AWGN) channel with SNR 0 dB, (2) AWGN channel with SNR -5 dB. We studied the ranging accuracy using four different methods where ranging was conducted using (1) only signals with linearly increasing sub-chirps (set-1), (2) only signals with linearly decreasing sub-chirps (set-2), (3) mean-measurement method and (4) with Doppler-velocity correction method. The attenuation of the ultrasonic signal in the air was modeled as $A = A_0 e^{-\gamma \times d}$, where A, A_0 and d are the amplitude after attenuation, the originally transmitted amplitude and the distance from transmitter respectively. The attenuation constant γ was set to 0.17 Np/m. The mean values of the standard deviation of range errors for simulations with maximum Doppler-velocity of 1 m/s and four mobile nodes are

TABLE I
MEAN OF STANDARD DEVIATION OF RANGING ERRORS (IN MM) WITH ONLY SIGNALS FROM SET-1, SET-2, MEAN-MEASUREMENT METHOD (M-1) AND DOPPLER-VELOCITY CORRECTION METHOD (M-2) USING FOUR MOBILE NODES.

Type	Method	Node1	Node2	Node3	Node4
Simulation with 0 dB SNR	Set-1	82.74	83.88	75.13	80.94
	Set-2	83.21	76.20	80.99	80.70
	M-1	28.36	25.39	22.87	27.72
	M-2	15.43	13.21	12.22	14.34
Simulation with -5 dB SNR	Set-1	88.02	88.44	77.60	85.53
	Set-2	87.31	78.99	84.83	83.98
	M-1	35.01	30.82	27.90	33.03
	M-2	18.92	17.31	15.63	17.27

TABLE II
MEAN OF STANDARD DEVIATION OF RANGING ERRORS (IN MM) WITH ONLY SIGNALS FROM SET-1, SET-2, MEAN-MEASUREMENT METHOD (M-1) AND DOPPLER-VELOCITY CORRECTION METHOD (M-2) USING SIX MOBILE NODES.

Type	Method	Node1	Node2	Node3	Node4	Node5	Node6
Simulation with 0 dB SNR	Set-1	114.95	105.74	87.8	82.29	94	88.27
	Set-2	107.71	94.72	87.83	90.49	86.38	69.95
	M-1	71.53	62.93	52.12	51.31	54.4	45.94
	M-2	49.38	38.67	28.79	29.66	26.94	25.95
Simulation with -5 dB SNR	Set-1	131.19	119.91	98.66	94.69	106.07	99.19
	Set-2	122.64	106.77	99.39	103.5	100.64	79.05
	M-1	84.22	73.8	62.35	62.28	65.63	55.1
	M-2	60.59	46.89	36.57	38.68	35.32	32.34

provided in Table I. It can be observed that we are able to get less than 20mm accuracy in all the cases using the Doppler-velocity correction method in scenario-1. For scenario-2 with six number of mobile nodes, we did the same experiments to quantify the effect of increase in multiple access interference. The results are provided in Table II. It can be observed that as the number of transmitters increases, the error also increases. The errors using the proposed methods are much lesser than that of using only set-1 or set-2 signals even though the error increased more in the proposed methods when multiple access interference was increased. To find the dependence of error on the maximum simulated Doppler-velocity, we changed the maximum Doppler-velocity in scenario-1 with 0dB SNR. The average number of error in the estimated range exceeding ± 20 mm was plotted against the maximum simulated Doppler-velocity in Fig. 7. As the velocity is increased, the error in the range measurements using Doppler-velocity correction method increases much slower compared to the mean-measurement method. The velocity estimated from the Doppler-velocity correction method for one mobile node is compared with the actual velocity in Fig. 8. It shows that the proposed method can track the Doppler-velocity quite accurately. The plots of the range estimated from signals using set-1, set-2 and Doppler-velocity correction method are shown in Fig. 9. It can be observed that the range estimated using set-1 and set-2 signals are shifted from the actual range due to the range-Doppler coupling. To summarize, the Doppler-velocity correction method performed better followed by the mean-measurement method for ultrasonic ranging with four and six number of transmitters using a narrow bandwidth of 4 kHz and 6 kHz respectively.

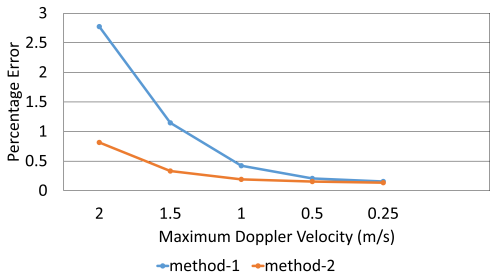

Fig. 7. Percentage of absolute ranging error greater than 20 mm as maximum simulated Doppler-velocity is varied in a wireless channel with 0 dB Gaussian noise

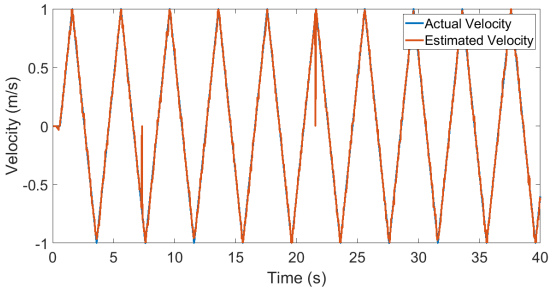

Fig. 8. Comparison of estimated Doppler-velocity from Doppler-velocity correction method with the actual simulated velocity of one mobile node with 0 dB Gaussian noise for scenario-1.

VI. EXPERIMENTAL PROCEDURE

A pendulum experiment was designed to test the proposed method on hardware using narrowband ultrasonic sensors with a centre frequency of 40 kHz. We selected MA40S4S and MA40S4R from MURATA as transmitters and receiver respectively. The transmitters and the receiver were connected to NI-USB 6343 Data Acquisition (DAQ) board which was connected to the PC through USB. DAQ board drives sensors at 10v. Since the sensors used in this experiment works with low voltages (<20v), wireless sensor nodes with ADCs, wireless clock synchronization and batteries can replace this setup to reduce cost without considerable degradation in the ranging performance in the future [1]. Four ultrasonic transmitters were attached on a pendulum with about 120 mm distance between adjacent sensors. The hinge of the pendulum was kept about 1300 mm above the floor level. The first, second, third and the fourth transmitters were placed at a distance

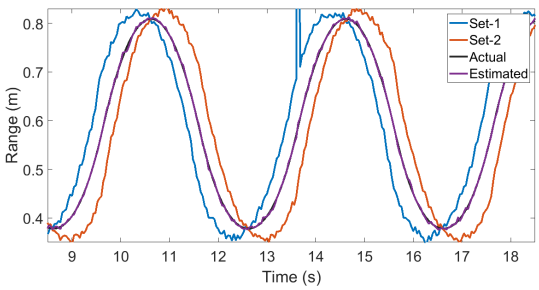

Fig. 9. The range estimated from the simulation experiment using signals from set-1, set-2 and Doppler-velocity correction method and the actual range at a simulated Doppler-velocity of 1m/s.

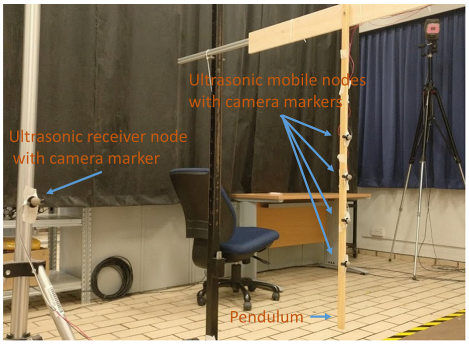

Fig. 10. The pendulum setup with multiple ultrasonic transmitters attached and one static receiver.

of 760, 640, 520 and 400 mm from the hinge. A set of optimized signals from set-1 and set-2 are transmitted through the transmitters attached on a pendulum as shown in Fig. 10 while the pendulum was made to swing. The ranging was conducted with the receiver placed at eight different positions so that the distance between the pendulum and the receiver lies in between 500 to 1500m. The orientation of the receiver was also changed a little bit each time without affecting the LOS. The experiments were conducted at Motion Analysis Laboratory, Nanyang Technological University, Singapore. Eagle motion capture system with six high-speed infrared cameras was used as the reference system. Reflective markers were placed adjacent to the ultrasonic transmitters and the receiver. The motion capture system was calibrated before the experiments and the accuracy of the system was found to be 0.36 ± 0.17 after calibration. The pendulum was released from about $45°$ from the vertical position after both systems are started. The range measurements were recorded for about 16 seconds. This experiment was repeated eight times and the mean value of the standard deviation between the range values extracted from ultrasonic sensors and the motion capture system was found out. To filter out large errors which lie outside our range, we used a pre-filtering step in which a range measured was considered as a valid measurement only if the range estimated from both set-1 and set-2 corresponding to the sampling point lies in our range of interest.

VII. Results and Discussions

We aimed to test whether orthogonally coded chirp signals can be used for accurate tracking and simultaneous Doppler correction without using a bank of matched filters at the receiver side for indoor tracking applications. The results from the pendulum experiment are shown in Table III. As expected, both the Doppler-velocity correction method and the mean-measurement method resulted in an improvement in the standard deviation between the proposed ranging system and the Motion capture system when compared to the results obtained from only set-1 or only set-2. The improvement in tracking performance is narrow as the Doppler-velocity experienced by the ultrasonic sensors during the pendulum experiment is very small, this is because the major part of movement happens in a direction perpendicular to the transmission direction of the ultrasonic wave. The range measurements obtained

TABLE III
The mean value of the Standard deviation of ranging errors (in mm) with only signals from set-1, set-2, mean-measurement method (M-1) and Doppler-velocity correction method (M-2) during the pendulum experiment

Method	Node1	Node2	Node3	Node4
Set-1	5.70	6.10	4.16	3.69
Set-2	6.19	6.09	3.83	3.69
M-1	5.68	5.08	3.74	3.39
M-2	5.69	5.04	3.74	3.39

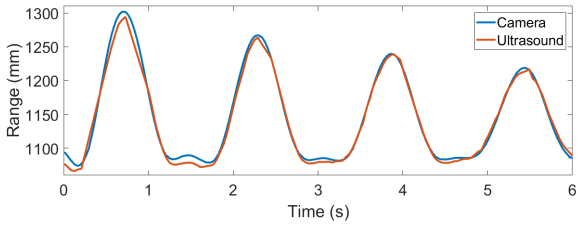

Fig. 11. Comparison of Range measurements from the camera system and the ultrasonic system with the proposed method during the pendulum experiment.

from the ultrasonic system using the proposed method and the motion capture system are compared in Fig. 11. The proposed method can be used to offset the errors brought about by the movement of mobile nodes in ultrasonic localization systems. Unlike accelerometers and gyroscopes, we do not need any integration to find the three-dimensional position for localization using ultrasonic ranging and hence the localization systems using this method can be exploited for long-duration tracking of moving targets. From the simulation results, we can find that the error does not increase much using Doppler-velocity correction method as the maximum Doppler-velocity was increased from 0.25 to 2 m/s. In both methods, two number of correlations need to be conducted to estimate one sample point. The second method also includes calculation of Doppler-velocity which is not computationally intensive. We compare the complexity with [20], [24] where a bank of matched filters are needed and more than two correlations need to be conducted to estimate one sample point. The maximum Doppler-velocity and the capture volume have limitations in this system. The range of ultrasonic sensors used was 0.2 to 4 m. In the simulation experiments, we subjected the sensors to a maximum Doppler-velocity of 1 m/s and got good tracking performance. However, the maximum Doppler-velocity, the system can withstand, depends on the multi-path effect, number of transmitters and the available bandwidth. In our experiments with sensors, we subjected small Doppler velocities less than 0.5 m/s as the movement was parallel to the receivers for maintaining LOS. In our experiments, as the distances between different ultrasonic transducers are not very large, we did not face near-far effect ([26], [27]), as the nodes were facing each other and the distance between them was small. This problem, along with higher Doppler velocities, needs to be tested in future experiments.

VIII. Conclusion and Future work

Two methods for ultrasonic ranging between multiple slow-moving ultrasonic transducers with Doppler shift compen-

sation are proposed. Orthogonally coded linearly increasing and decreasing chirp signals were employed for ranging. Simulation results show that the proposed method can enhance the performance of small-scale ultrasonic ranging. The Doppler-velocity compensation method outperformed the mean-measurement method in the simulation results as the former accounts for the modification of linear chirp by the Doppler effect. A pendulum experiment was conducted using narrowband ultrasonic sensors and we obtained an improvement in the ranging accuracy at lower moving velocities using the proposed methods.

In the future, the system can be implemented for localization and motion tracking applications such as gait analysis. We plan to conduct experiments at higher Doppler velocities using methods to increase the transmission angle of the transducers. The effects of changes in multi-path conditions, the near-far effect on the ranging performance and the correction methods are also a potential area of study.

REFERENCES

[1] K. Ashhar, M. Khyam, C. Soh, and K. Kong, "A doppler-tolerant ultrasonic multiple access localization system for human gait analysis," *Sensors*, vol. 18, no. 8, p. 2447, 2018.

[2] R. Zhang, F. Höflinger, and L. Reindl, "Tdoa-based localization using interacting multiple model estimator and ultrasonic transmitter/receiver," *IEEE Transactions on Instrumentation and Measurement*, vol. 62, no. 8, pp. 2205–2214, 2013.

[3] S. J. Kim and B. K. Kim, "Dynamic ultrasonic hybrid localization system for indoor mobile robots," *IEEE Transactions on Industrial Electronics*, vol. 60, no. 10, pp. 4562–4573, 2013.

[4] S. Zhou, F. Fei, G. Zhang, J. D. Mai, Y. Liu, J. Y. Liou, and W. J. Li, "2d human gesture tracking and recognition by the fusion of mems inertial and vision sensors," *IEEE Sensors Journal*, vol. 14, no. 4, pp. 1160–1170, 2014.

[5] J. D. Hol, F. Dijkstra, H. Luinge, and T. B. Schon, "Tightly coupled uwb/imu pose estimation," in *Ultra-Wideband, 2009. ICUWB 2009. IEEE International Conference on*. IEEE, 2009, pp. 688–692.

[6] D. Roetenberg, H. Luinge, and P. Slycke, "Xsens mvn: full 6dof human motion tracking using miniature inertial sensors," *Xsens Motion Technologies BV, Tech. Rep*, vol. 1, 2009.

[7] R. Zhu and Z. Zhou, "A real-time articulated human motion tracking using tri-axis inertial/magnetic sensors package," *IEEE Transactions on Neural systems and rehabilitation engineering*, vol. 12, no. 2, pp. 295–302, 2004.

[8] M. O. Khyam, M. J. Alam, A. J. Lambert, M. A. Garratt, and M. R. Pickering, "High-precision ofdm-based multiple ultrasonic transducer positioning using a robust optimization approach," *IEEE Sensors Journal*, vol. 16, no. 13, pp. 5325–5336, 2016.

[9] M. R. Mahfouz, C. Zhang, B. C. Merkl, M. J. Kuhn, and A. E. Fathy, "Investigation of high-accuracy indoor 3-d positioning using uwb technology," *IEEE Transactions on Microwave Theory and Techniques*, vol. 56, no. 6, pp. 1316–1330, 2008.

[10] M. O. Khyam, M. Noor-A-Rahim, X. Li, C. Ritz, Y. L. Guan, and S. S. Ge, "Design of chirp waveforms for multiple-access ultrasonic indoor positioning," *IEEE Sensors Journal*, vol. 18, no. 15, pp. 6375–6390, 2018.

[11] M. Toda, "Cylindrical pvdf film transmitters and receivers for air ultrasound," *IEEE transactions on ultrasonics, ferroelectrics, and frequency control*, vol. 49, no. 5, pp. 626–634, 2002.

[12] A. J. Martín, Á. H. Alonso, D. Ruíz, I. Gude, C. De Marziani, M. C. Pérez, F. J. Álvarez, C. Gutiérrez, and J. Ureña, "Emfi-based ultrasonic sensory array for 3d localization of reflectors using positioning algorithms," *IEEE Sensors Journal*, vol. 15, no. 5, pp. 2951–2962, 2015.

[13] R. J. Przybyla, S. E. Shelton, A. Guedes, I. I. Izyumin, M. H. Kline, D. A. Horsley, and B. E. Boser, "In-air rangefinding with an aln piezoelectric micromachined ultrasound transducer," *Ieee sensors journal*, vol. 11, no. 11, pp. 2690–2697, 2011.

[14] M. Hazas and A. Hopper, "Broadband ultrasonic location systems for improved indoor positioning," *IEEE Transactions on mobile Computing*, vol. 5, no. 5, pp. 536–547, 2006.

[15] L. Segers, J. Tiete, A. Braeken, and A. Touhafi, "Ultrasonic multiple-access ranging system using spread spectrum and mems technology for indoor localization," *Sensors*, vol. 14, no. 2, pp. 3172–3187, 2014.

[16] M. M. Saad, C. J. Bleakley, T. Ballal, and S. Dobson, "High-accuracy reference-free ultrasonic location estimation," *IEEE Transactions on Instrumentation and Measurement*, vol. 61, no. 6, pp. 1561–1570, 2012.

[17] M. Alloulah and M. Hazas, "An efficient cdma core for indoor acoustic position sensing," in *Indoor Positioning and Indoor Navigation (IPIN), 2010 International Conference on*. IEEE, 2010, pp. 1–5.

[18] O. A. Aly and A. Omar, "Spread spectrum ultrasonic positioning system," in *Proceedings of the 2nd Workshop on Positioning, Navigation and Communication (WPNC05), Magdeburg, Germany*, 2005, pp. 109–114.

[19] P. Misra, N. Kottege, B. Kusy, D. Ostry, and S. Jha, "Acoustical ranging techniques in embedded wireless sensor networked devices," *ACM Transactions on Sensor Networks (TOSN)*, vol. 10, no. 1, p. 15, 2013.

[20] F. J. Álvarez, Á. Hernández, J. A. Moreno, M. C. Pérez, J. Ureña, and C. De Marziani, "Doppler-tolerant receiver for an ultrasonic lps based on kasami sequences," *Sensors and Actuators A: Physical*, vol. 189, pp. 238–253, 2013.

[21] M. O. Khyam, S. S. Ge, L. Xinde, and M. Pickering, "Mobile ultrasonic transducer positioning," *The Journal of Engineering*, vol. 2017, no. 4, pp. 119–122, 2017.

[22] R. J. Fitzgerald, "Effects of range-doppler coupling on chirp radar tracking accuracy," *IEEE Transactions on Aerospace and Electronic Systems*, no. 4, pp. 528–532, 1974.

[23] W.-Q. Wang, "Mimo sar chirp modulation diversity waveform design," *IEEE Geoscience and Remote Sensing Letters*, vol. 11, no. 9, pp. 1644–1648, 2014.

[24] P. Misra, "Acoustical localization techniques in embedded wireless sensor networked devices," Ph.D. dissertation, Ph. D. Dissertation. University of New South Wales, 2012.

[25] H. Lee, T. H. Kim, J. W. Choi, and S. Choi, "Chirp signal-based aerial acoustic communication for smart devices," in *Computer Communications (INFOCOM), 2015 IEEE Conference on*. IEEE, 2015, pp. 2407–2415.

[26] F. Seco, J. C. Prieto, A. R. J. Ruiz, and J. Guevara, "Compensation of multiple access interference effects in cdma-based acoustic positioning systems," *IEEE Transactions on Instrumentation and Measurement*, vol. 63, no. 10, pp. 2368–2378, 2014.

[27] M. Khyam, L. Xinde, S. S. Ge, and M. R. Pickering, "Multiple access chirp-based ultrasonic positioning," *IEEE Transactions on Instrumentation and Measurement*, vol. 66, no. 12, pp. 3126–3137, 2017.

K. Ashhar received the Bachelor of Technology in Electronics and Communication Engineering from National Institute of Technology Calicut, India in 2013. He is currently a Ph.D. student in School of Electrical and Electronic Engineering in Nanyang Technological University, Singapore. His current research interest is in biomedical signal processing, sensors, localization with ultrasonic sensors and motion tracking for rehabilitation and gait analysis

Md. Noor A Rahim received his Ph.D. degree from Institute for Telecommunications Research, University of South Australia, Australia in December 2015. He is currently a Marie-Curie Research Fellow at the CONNECT Research Centre, Ireland. Previously, he was a Post-doctoral Research Fellow at the Centre for Infocomm Technology (INFINITUS), Nanyang Technological University (NTU), Singapore. He is the recipient of Michael Miller Medal for the most outstanding Ph.D. thesis in 2015 from the Institute for Telecommunications Research (ITR), University of South Australia. His research interests include information theory, wireless communications, and vehicular communications.

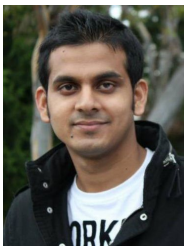

Mohammad Omar Khyam received the B.Sc. degree in electronics and telecommunication engineering from the Rajshahi University of Engineering and Technology, Rajshahi, Bangladesh, in 2010, and the Ph.D. degree from the University of New South Wales, Australia, in 2015. He is currently a Post-Doctoral Research Fellow with the Virginia Tech, VA, USA. His research interests include signal processing and wireless communication.

Cheong Boon Soh (M84 - SM03) received the Bachelor of Engineering in Electrical and Computer Systems Engineering (Hons I) and PhD degrees from Monash University, Victoria, Australia, in 1983 and 1987, respectively. He is an Associate Professor in the School of Electrical and Electronic Engineering, Nanyang Technological University, Singapore. He has published more than 120 international journal papers. His current research interests are ultrawideband (UWB) for medical applications, auscultation and stroke assessment, E-medicine, robust control, system theory, nonlinear systems, coding theory, networking, mobile communication systems and intelligent systems.